

Effect of temperatures on anaerobic granulated biofilm modelling

Anissa Sukma Safitri^a and Roald Kommedal^a

^a *Institute of Chemistry, Bioscience and Environmental Engineering, University of Stavanger, 4036 Stavanger, Norway*
Email: anissa.s.safitri@uis.no and roald.kommedal@uis.no

Abstract

Anaerobic granulated biomass-based treatment is a sustainable alternative for municipal wastewater treatment. Each granule in the system is comprised of a complex community of anaerobic microorganisms embedded in a biofilm matrix. The aim of this work was to implement a biofilm model for simulation of biogas production and COD removal as observed in an experimental up-flow anaerobic sludge blanket (UASB) reactor system. Additionally, selected scenario simulations were carried out to assess the effect of temperatures (25, 16, and 12 °C) on granulated anaerobic reactor performance at different organic loading rates. The two main model components used are: Dynamic biochemical and physicochemical conversion processes (Anaerobic Digestion Model No. 1) and diffusive mass transfer within the granule (biofilm). The model was implemented in AQUASIM 2.1. Simulations gave insight into non-observables, especially intragranular biomass distribution and substrate profiles, which help our understanding of granule formation and evolution. Results reflected observed effluent COD concentrations and methane production rates at variable temperatures and reactor loadings. Simulations also confirmed observed steady-state reductions in COD removal efficiencies and methane fraction in biogas at increasing organic loading rate. Model simulations also showed intra-granular alkaline pH depth profiles with increasing organic loading rate which may explain calcium-based mineral core formation. The biomass composition and active regions in granules were not significantly affected by organic loading rate. At steady state, organic substrates especially monosaccharides and volatile fatty acids were predicted to degrade approximately within the outer 100 µm. In general, the model can be used as a tool to predict and simulate anaerobic granulated biofilm system performances in UASB reactor.

Keywords: Anaerobic granule; Biofilm modelling; Municipal wastewater

1. Introduction

Mathematical bioprocess modelling is a recognized tool for fundamental bioprocess understanding, data analysis and hypothesis testing, for design and optimization of wastewater treatment processes (Henze et al., 2008). Considerable efforts has been dedicated for the development of mathematical models for anaerobic granular technology, recently summarized by Baeten et al. (2019). Two main approaches are used for anaerobic granular modelling: The intragranular transport models (biofilm models) and the suspended biomass liquid phase models using apparent kinetics. Granular biofilm models are used for any redox system, while the apparent kinetic models are more commonly used for anaerobic systems (Baeten et al., 2019). In biofilm reactors, substrate transport from the bulk liquid into the microbial matrix is normally controlled by diffusion. Wanner & Gujer (1986) identified several beneficial objectives attainable by using biofilm models: Understanding the

mechanisms fundamental to how a biofilm forms or performs; integration of different mechanisms occurring at different spatial and temporal scales; pre-model the system to generate expected results; and evaluating novel process designs.

The Anaerobic Digestion Model no. 1 (ADM1) is recognized as the standard model for conversion of organic substrates to biogas in open wastewater and biosludge systems (Batstone et al., 2002). Bioconversion, physicochemical reactions, and interface mass transfer are combined into a model comprising the most important state variables and processes. In addition, bioconversion parameters under typical anaerobic meso- to thermophilic conditions are suggested.

Biofilm models of anaerobic granules under mass transfer limitations and single as well as multiple limiting substrates are available in the literatures (Batstone et al., 2004; Buffière et al., 1995; Doloman et al., 2020; Feldman et al., 2017; Flora et

al., 1995; Odriozola et al., 2016; Sun et al., 2016). Granulated biofilm models have been implemented on several platforms, such as AQUASIM (Batstone et al., 2004) and MATLAB (Odriozola et al., 2016). Extension of the strictly suspended/homogenous ADM1 into a biofilm setting require diffusive transport for all dissolved components, attachment/detachment mechanisms for particulates and possibly moderation of kinetic and/or stoichiometric coefficients for the growth-related conversions. As for the latter, the work of Bakke et al. (1984) suggest that conversion kinetics are not significantly moderated by a biofilm phenotypic growth state, but possibly the stoichiometry due to EPS formation and degradation (Kommedal et al., 2001). Physio-chemical mass transfer parameters are available in the physical chemical reference literature.

The aim of this work was to propose a biofilm model relevant for an anaerobic granule typical of an up-flow anaerobic sludge blanket (UASB) reactor system. The proposed model was evaluated by simulation of experimental observations in a laboratory scale UASB reactor receiving strong municipal wastewater. Additionally, analyses were carried out to assess the effect of temperatures (25, 16, and 12 °C) on granulated anaerobic reactor performance at different organic loadings and compare these to experimental results.

2. Methodology

2.1. Experimental set-up and results

A long-term operation of up-flow anaerobic sludge blanket (UASB) system treating real municipal wastewater from IVAR IKS, Norway, at decreasing temperatures (25, 16, 12, 8.5, 5.5, and 2.5 °C) and variable organic loading rates (OLR) from 1.0 $\text{gCOD}\cdot\text{l}^{-1}\cdot\text{d}^{-1}$ up to 15.2 $\text{gCOD}\cdot\text{l}^{-1}\cdot\text{d}^{-1}$ was investigated over 1025 days (Figure 1). Experiments were performed in two parallel in-house designed laboratory-scale UASB reactors, which were operated continuously with hydraulic retention time (HRT) of 16.7 h down to 1.1 h. The wastewater may be characterized as a municipal wastewater with significant contributions from agricultural and food industries. The dissolved COD concentrations of inlet wastewater during UASB reactor operation fluctuated in the range 439 - 1473 $\text{mgCOD}_{\text{dissolved}}\cdot\text{l}^{-1}$ with the mean concentration being 741 ± 7 $\text{mgCOD}_{\text{dissolved}}\cdot\text{l}^{-1}$ (\pm standard error).

Stable COD removal efficiencies of 50 - 70 % were achieved at 25 °C down to 8.5 °C with loading up to approximately 15.2 $\text{gCOD}\cdot\text{l}^{-1}\cdot\text{d}^{-1}$. COD removal efficiencies were reduced at temperatures below 8.5 °C, but significant methane formation was observed even at 2.5 °C at reduced loading (up to 5 $\text{gCOD}\cdot\text{l}^{-1}$

$\cdot\text{d}^{-1}$). More than 90% of COD removed was converted to methane. The overall COD balance closed at above 90% of the inlet COD at all operating temperatures and OLRs. Temperature affected the reactor performances, microbial community structure, and the degradation pathway of organic matter with acetoclastic methanogen and methylotrophic played significant roles (Safitri et al., 2022).

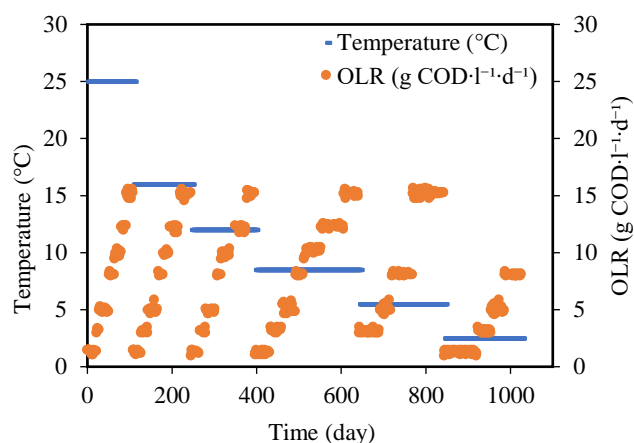


Figure 1 The UASB reactors were operated continuously over 1025 days by the stepwise increase of OLR at decreasing temperatures.

2.2. Model implementation

The biomass in UASB systems is in the form of compact granules that contain a complex community of microorganisms embedded in the extracellular polymeric substances (EPS) matrix, i.e., biofilm. This presented model used to predict the behavior of a granule biofilm representative of the UASB reactor described in section 2.1. For simplification, scenario analyses were carried out to assess the effect of temperatures (25, 16, and 12 °C) on reactor performances, as shown in Figure 2.

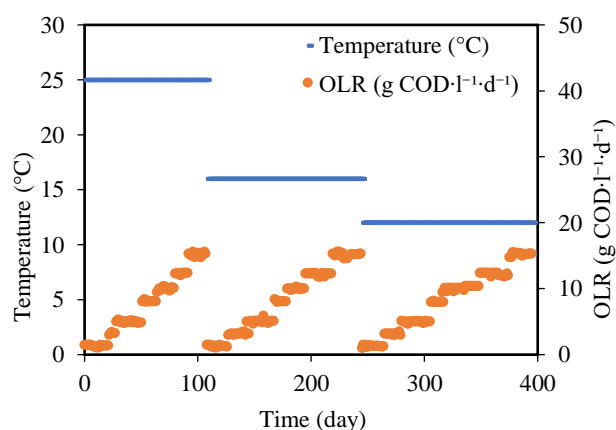


Figure 2 Simulation scenario in biofilm modelling by the stepwise increase of OLR at decreasing temperatures.

The two main model structures implemented are: Biochemical and physico-chemical conversion

processes as described in the Anaerobic Digestion Model No. 1 (ADM1) by Batstone et al. (2002) and diffusive mass transfer model for granulated biomass (the biofilm compartment) based on Wanner and Gujer (1986). The biochemical conversions included: a. Disintegration of particulates to biopolymers (polysaccharides, proteins, and lipids); b. hydrolysis of biopolymers to sugars, amino acids, and long-chain fatty acids (LCFA); c. acidogenesis from sugars and amino acids to volatile fatty acids (VFAs) and hydrogen; d. acetogenesis of LCFA and VFAs to acetate; and e. separate methanogenesis steps from acetate and hydrogen/CO₂ (Hulshoff Pol et al., 2004). The physico-chemical equations describe ion association and dissociation, and gas-liquid mass transfer. Inhibition kinetics have been integrated in relevant biochemical process.

The diffusion limited biogeochemical model was implemented in AQUASIM 2.1 (Reichert, 1994). The ADM1 conversions were implemented in the biofilm compartment using 20 vertical grid points evenly distributed over the biofilm depth. The bulk liquid is modelled as a mixed reactor, with liquid borne in- and out-fluxes and bulk liquid biochemical reactions equal to the biofilm matrix reactions. An additional mixed compartment was implemented to represent the gas phase, connected by a diffusive link to simulate the gaseous transfer of methane, carbon dioxide, and hydrogen. Figure 3 presents the schematic of the biofilm compartment implementation.

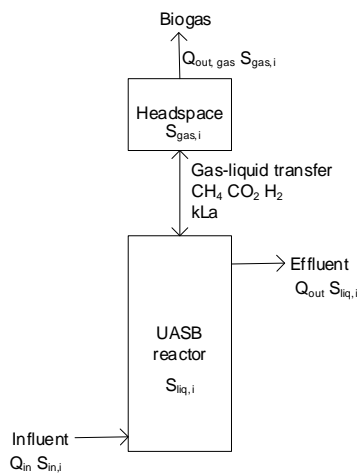


Figure 3 Schematic representation of anaerobic granulated biofilm implementation into ADM1

Acid-base reactions in the ADM1 model can either be implemented as a combination of differential and algebraic sets of equations (DAE) or by fast time dependent differential equations (DE). The standard (commonly available) ADM1 simulators implemented for CSTR (using AQUASIM 2.1) use

the DAE approach. However, herein the acid-base biofilm model is implemented by solving individual acids and conjugated bases separately, as dynamic state variables. All ionic species were implemented as differential variables and a pH model construction followed a step-by-step procedure based on Hofmann et al. (2008). The following Equation 1 for calculating hydrogen ion concentration was used:

$$S_{H^+} = -\frac{\theta}{2} + \frac{1}{2}\sqrt{\theta^2 + 4K_w} \quad (\text{Equation 1})$$

where θ is the net charge in the system resulting from all acid-bases considered in the model:

$$\theta = S_{CAT} + S_{NH_4^+} + S_{H^+} - \frac{S_{AC^-}}{64} - \frac{S_{PRO^-}}{112} - \frac{S_{BU^-}}{160} - \frac{S_{VA^-}}{208} - S_{HCO_3^-} - \frac{K_w}{S_{H^+}} + -S_{AN}$$

As stated by the Stokes-Einstein equation, the diffusion coefficient in water (D_{aq}) depends on temperature, both directly and through the effect of temperature (T) on the solution viscosity (μ) (Cussler, 1984). This temperature dependence of aqueous diffusion coefficients can be calculated through the relationship in Equation 2.

$$\frac{D_{aq} \mu}{T} = \text{constant} \quad (\text{Equation 2})$$

The value of the effective diffusion coefficient in the biofilm ($D_{aq,e}$) will be reduced compared to the diffusion coefficient in water due to the presence of microbial cells, extracellular polymers, and abiotic particles or gas bubbles that are trapped in the biofilm (Stewart, 2003). This reduction is described by the ratio $D_{aq,e}/D_{aq}$ (Equation 3). The diffusion coefficients in water (D_{aq}) at 25 °C were taken from Cussler (1984) and Stewart (1998). Effective diffusivities ($D_{aq,e}$) used in current biofilm model (Table 1) were calculated using Equation 2 and 3 with correction to 16 and 12 °C. The solution viscosity (μ) of water at different temperatures were adapted from Coulson & Richardson (1999).

Table 1 Effective diffusivities used in current biofilm model

Variables	$D_{aq,e}/D_{aq}^a$	$D_{aq,e}$ at different temperature ($\times 10^{-5} \text{ m}^2 \cdot \text{d}^{-1}$)		
		25 °C	16 °C	12 °C
Effective diffusivity:				
Amino acids	0.40	2.63	2.05	1.81
Acetate	0.21	2.20	1.71	1.51
Butyrate	0.34	2.56	1.99	1.76
Methane	0.40	5.15	4.02	3.55
CO ₂	0.40	6.64	5.18	4.58
LCFA	0.20	1.62	1.27	1.12
Hydrogen	0.60	23.33	18.20	16.10
Cations/anions	0.49	5.00	3.90	3.45
Ammonia	0.75	10.63	8.29	7.33
Propionate	0.30	2.75	2.14	1.90
Soluble inerts	0.10	0.86	0.67	0.59
Sugar/glucose	0.30	1.74	1.35	1.20
Valerate	0.30	0.50	0.39	0.35

^aReferences: Cussler (1984) and Stewart (1998)

Modified kinetics of the particulate first order disintegration constant (k_{dis}), first order hydrolysis constant (k_{hyd}) and maximum uptake rates (k_m) at different temperatures were retrieved and estimated from literatures (Bergland et al., 2015; Donoso-Bravo et al., 2009; Lohani et al., 2018; Rebac et al., 1995). The temperature compensated kinetic values at 25, 16 and 12 °C were presented in Table 2, taking 35 °C as the reference condition (Batstone et al., 2004).

Table 2 Kinetic parameters k_{dis} , k_{hyd} , k_m with temperature

Process	Temperature (°C)			
	35 ^a	25 ^b	16 ^b	12 ^b
Disintegration (k_{dis} , d ⁻¹)	0.5	0.24	0.07	0.06
First order hydrolysis (k_{hyd} , d ⁻¹):				
Carbohydrate	106	51	15	13
Protein	2.7	1.3	0.4	0.3
Lipid	0.40	0.19	0.06	0.05
Maximum uptake rates (k_m , d ⁻¹):				
Sugars	150	32	24	24
Amino acids	250	53	40	40
Fatty acids	30	6.3	4.8	4.8
Butyrate	100	67	36	23
Propionate	65.0	45.5	18.9	10.4
Acetoclastic methanogens	40.0	27.6	8.0	6.0
Hydrogenotrophic methanogens	175	120.8	35.0	26.3

References:

^aRetrieved from Batstone et al. (2004)

^bEstimated from literatures (Bergland et al., 2015; Donoso-Bravo et al., 2009; Lohani et al., 2018; Rebac et al., 1995)

Physico-chemical equilibria are modeled based on the law of mass action for aqueous substances and by Henry's law for the solubility of a gas. Table 3 presents temperature dependent physico-chemical processes parameters used in biofilm modelling. Detailed calculations and model source file are available on request from the authors.

Table 3 Temperature dependent physico-chemical processes parameters

Description	Temperature compensation	References
Acidity constants (K_a):		
CO ₂	$10^{-6.35} \exp\left(\frac{7646}{100 \cdot R} \cdot \left(\frac{1}{T_{std}} - \frac{1}{T}\right)\right)$	Lide (2003)
H ₂ O	$10^{-13.995} \exp\left(\frac{55900}{100 \cdot R} \cdot \left(\frac{1}{T_{std}} - \frac{1}{T}\right)\right)$	Lide (2003)
NH ₄ ⁺	$10^{-9.25} \exp\left(\frac{51965}{100 \cdot R} \cdot \left(\frac{1}{T_{std}} - \frac{1}{T}\right)\right)$	Lide (2003)
Henry's law constants (K_H):		
CH ₄	$0.00140 \cdot R \cdot T \cdot \exp\left(\frac{-14240}{100 \cdot R} \cdot \left(\frac{1}{T_{std}} - \frac{1}{T}\right)\right)$	Batstone et al. (2002)
CO ₂	$0.03400 \cdot R \cdot T \cdot \exp\left(\frac{-7646}{100 \cdot R} \cdot \left(\frac{1}{T_{std}} - \frac{1}{T}\right)\right)$	Batstone et al. (2002)
H ₂	$0.00078 \cdot R \cdot T \cdot \exp\left(\frac{-4180}{100 \cdot R} \cdot \left(\frac{1}{T_{std}} - \frac{1}{T}\right)\right)$	Lide (2003)
Pressure of water	$0.0313 \cdot \exp\left(5290 \cdot \left(\frac{1}{T_{std}} - \frac{1}{T}\right)\right)$	Rosen and Jeppsson (2006)

2.3. Simulation set-up

The simulated reactor model consisted of a liquid (0.8 l) and a gas phase (0.2 l). The biofilm compartment corresponded to experimental data from this work (Safitri et al., 2022) and consisted of approximately 300 ml of granular sludge of an average uniform spherical granules with a diameter of 2 mm. The number of granules ($n_{sp} \approx 21500$) was calculated based on the total granule volume. Granules were assumed to have no dispersive solid transport (rigid biofilm matrix) and no suspended solids within biofilm matrix pores (pore volume contains only liquid phase). External mass transfer limitation was for simplicity reasons neglected (no diffusion limitations in the stagnant surface layer). Based on the above assumptions, this gave a total reactor biofilm surface area of 1.08 m². Detachment of biomass (Equation 4) is based on the non-linear biofilm thickness dependency proposed by Stewart et al. (1996):

$$r_{det} = k_{det} \cdot L_f^2 \quad (\text{Equation 4})$$

where k_{det} is an empirical detachment coefficient, (here: 0.024 kg·m⁻²·d⁻¹), and L_f is the simulated biofilm thickness (m). Biomass density within the granules was set at 180 kgCOD·m⁻³, a typical anaerobic granules density based on Batstone and Keller (2001).

Initial conditions were defined for the biofilm matrix and the bulk liquid volume as follows: All modelled microorganisms were considered to have equal initial bulk phase concentrations of 0.05% v/v (9 kgCOD·m⁻³) equal to the biomass fractions in the biofilm matrix. The initial biofilm thickness was set at 0.03 mm and bulk phase initial biomass, initial VFAs and pH was chosen among typical observed values at 10⁻⁵ kgCOD·m⁻³, 10⁻⁶ kgCOD·m⁻³ and 10⁻⁷ kmol·m⁻³, respectively. Approximate steady-state pore and bulk liquid concentrations were used as initial state variables. Simulation time was limited to 400 days, with a time resolution of 0.1 d and a numerical maximum time step limited to 4000 d.

2.4. Input characteristics

The COD influent to the UASB reactor is defined in the model as presented in Table 4 and were assumed to be primarily polysaccharides, proteins, and fats, taking into consideration that IVAR Grødalund wastewater treatment plant receives wastewater from food, animal, and dairy industries. A feed bicarbonate alkalinity of 0.01 M and inorganic nitrogen of 0.007 M were used which were in line with analysis of the wastewater applied in the UASB laboratory experiment.

Table 4 COD input used for simulations

Description	Fraction	Value	Unit
Amino acid	0.002	0.003	kg COD·m ⁻³
Acetic acid	0.08	0.1	kg COD·m ⁻³
Butyrate	0.08	0.1	kg COD·m ⁻³
Propionate	0.08	0.1	kg COD·m ⁻³
Valerate	0.08	0.1	kg COD·m ⁻³
LCFA	0.14	0.175	kg COD·m ⁻³
Sugar	0.1	0.075	kg COD·m ⁻³
Soluble inert	0.07	0.088	kg COD·m ⁻³
Carbohydrate	0.1	0.125	kg COD·m ⁻³
Protein	0.1	0.15	kg COD·m ⁻³
Lipid	0.1	0.15	kg COD·m ⁻³
Particulate inert	0.06	0.075	kg COD·m ⁻³
Composite/complex	0.005	0.006	kg COD·m ⁻³
Input total COD	1.00	1.26	kg COD·m ⁻³

3. Results and Discussions

Figure 4 presents simulated and observed COD effluent concentrations of the UASB reactor at 25, 16 and 12 °C. Simulated dissolved COD effluent concentration was close to that observed results throughout the whole test period, even though there were slightly differences especially at 12 °C. This might be interpreted as a to strong temperature compensation in the ADM1 model, or a change/adaptation in community structure towards low mesophilic bacteria.

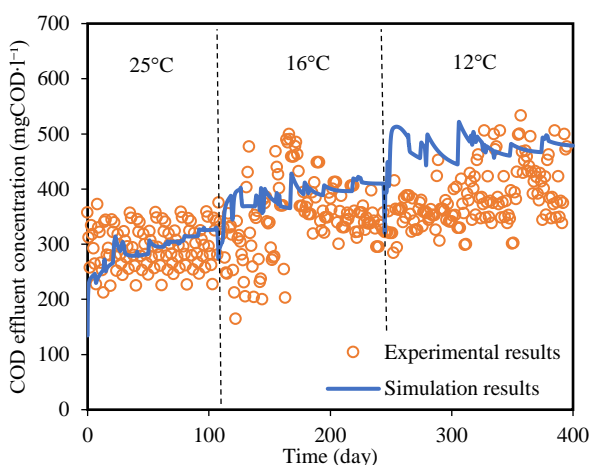


Figure 4 Simulated (blue dots) and measured (orange dots) COD effluent concentration profile in UASB reactor

Both simulation and experimental results show decreasing dissolved COD removal efficiencies at steady-state conditions with decreasing temperatures, from approximately 65 - 70% at 25 °C to around 57 - 66% at 12 °C. The relatively small fraction of particles degraded in our simulations (10 - 24% removal efficiency) indicate hydrolysis to be rate-limiting.

In simulations, methane fractions in the biogas at steady-state conditions decreased with increasing OLR with the range of 80 - 90% (data not shown), a trend that could not be significantly observed in

experimental data (Safitri et al., 2022). The dissolved methane concentrations in the effluent (86, 110, and 117 mgCOD·l⁻¹) were mimicked by the simulation result and are in line with theoretical value of dissolved methane at 25, 16, and 12 °C, respectively (Liu et al., 2014).

Figure 5 shows simulated and observed methane production profile in the UASB reactor at different temperatures and loadings. At each temperature, methane production increased with the increasing OLR, proportional to the amount of organic matter removed in the UASB reactors. Methane production at 12 °C was comparable in all OLRs to 16 °C, indicating that the reduction in operating temperature to 12 °C did not negatively affect methane production. This implies that the biomass has compensated for the temperature reduction by adaptation, and the model is overcompensating for the temperature reduction as both methane production and effluent COD reduction is larger than simulated, we assume an early kinetics to be overcompensated, like a to low hydrolysis coefficient.

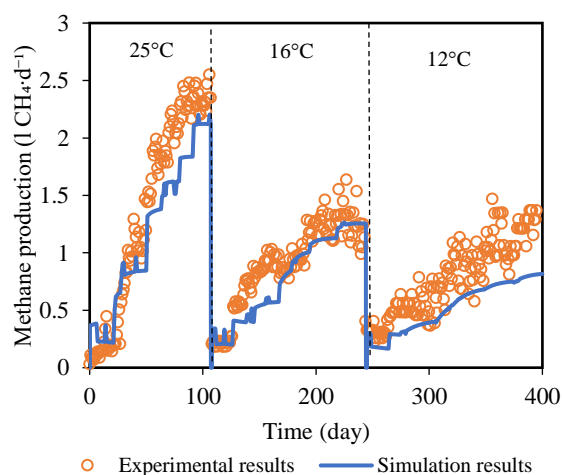


Figure 5 Simulated (blue dots) and measured (orange dots) methane production profile in UASB reactor

Considerable pH profile variations (approximately 7 - 8.3) through the depth of the granule were simulated as shown in Figure 6. The interior increase in pH inside the granules suggest calcium precipitation in the granule core. Amorphous CaPO₄, CaCO₃ and apatite precipitation (Ca₅(PO₄)₃OH) is known to stimulate granule formation, and could be exploited for phosphorous recovery (Cunha et al., 2018). Furthermore, simulated pH range in the bulk phase was about 7 which was comparable to observed pH (data not shown).

Simulated composition of granular sludge active biomass fractions for the experimental UASB

reactor is presented in Figure 7. Based on these results, methane production was mainly performed by acetoclastic methanogens at 25 °C, which dominated compared to hydrogenotrophic methanogens for all selected temperatures. However, hydrogenotrophic methanogens appeared more dominant at decreasing temperature at 12 °C.

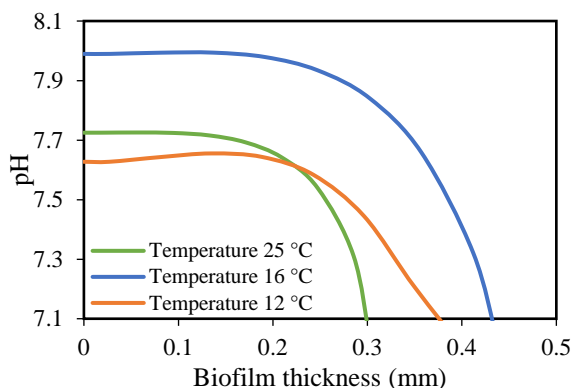


Figure 6 Simulated pH distribution profile along the granule in UASB reactor during steady-state conditions at different temperatures and OLR 15 gCOD·l⁻¹·d⁻¹.

Based on the experimental study, temperature affected the microbial community structure and the degradation pathway of organic matter with acetoclastic and methylotrophic methanogens played significant roles (Safitri et al., 2022). The original ADM1 model did not include methylotrophic methanogens which reduces the methyl-groups of methylated compounds to methane with H₂ as electron donor (Söllinger & Urich, 2019). Therefore, the simulated values are only to be qualitatively interpreted as they are not structurally comparable to experimental community analysis results.

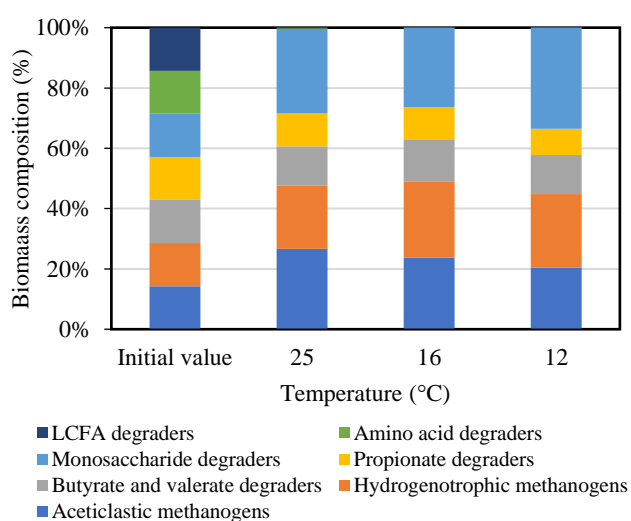


Figure 7 Simulated active biomass composition of the granular sludge of UASB reactor during steady-state conditions at different temperatures and OLR 15 gCOD·l⁻¹·d⁻¹.

According to simulation results, LCFA degraders only accounted for trace quantities of the active biomass. This could be explained by too low LCFA concentration to sustain biomass. There are significant decreases of amino acid degraders. However, more than 90% of the influent amino acid and LCFA was converted in the reactor at all temperatures. There is no significant temperature effect on bacterial distribution profile along the granule in UASB reactor during steady-state conditions. The sugar degraders had the highest concentration on the outer layer of granular sludge followed by butyrate and valerate degraders, hydrogenotrophic and acetoclastic methanogens.

The high amount of carbohydrates in the wastewater, supported these bacterial groups and resulted in a high methane concentration in the produced biogas. In the granules, the acetate degrading biomass peaked approximately 100 μm behind the biofilm-bulk boundary. Acetate concentrations were at their maximum at the biofilm boundary. The delayed front was possibly due to the faster growth of the other organisms, and a consequent high availability (not concentration) of acetate. Monosaccharide and VFA substrates are predicted to degrade approximately within the outer 100 - 200 μm. The granules had generally lower intermediate substrate concentrations than the bulk phase, indicating no net diffusive force out of the biofilm and intermediate reactions are not overloaded.

4. Conclusions

The proposed ADM1-biofilm model reflected the key effluent/bulk phase state variables as observed in the experimental UASB reactor system fed municipal wastewater. Furthermore, the model reflected the effect of reduced temperatures on overall COD conversion and biogas reactor performances at variable organic loading rates. The temperature compensation model used herein is too strong at 12 °C, maybe due to biomass adaptations. Available data are insufficient to validate the intra-granular state variables, but simulation results indicate ideal acid-base chemistry for inorganic granule core formation/growth.

Acknowledgment

The authors gratefully acknowledge the Norwegian Ministry of Education and Research through the university grant program (Norwegian Department of Education) and by the Foundation Stiftelsen Signe-Marie (<https://www.stiftelsensignemarie.no/>), for their support of this research project. We would like to acknowledge the wastewater treatment plant,

IVAR IKS, Norway, for practical support, wastewater logistics and operational advice.

References

- Baeten, J. E., Batstone, D. J., Schraa, O. J., van Loosdrecht, M. C. M., & Volcke, E. I. P. (2019). Modelling anaerobic, aerobic and partial nitrification-anammox granular sludge reactors—A review. *Water Research*, *149*, 322–341. <https://doi.org/10.1016/j.watres.2018.11.026>
- Bakke, R., Trulear, M. G., Robinson, J. A., & Characklis, W. G. (1984). Activity of *Pseudomonas aeruginosa* in biofilms: Steady state. *Biotechnology and Bioengineering*, *26*(12), 1418–1424. <https://doi.org/10.1002/bit.260261204>
- Batstone, D. J., & Keller, J. (2001). Variation of bulk properties of anaerobic granules with wastewater type. *Water Research*, *35*(7), 1723–1729. [https://doi.org/10.1016/S0043-1354\(00\)00446-2](https://doi.org/10.1016/S0043-1354(00)00446-2)
- Batstone, D. J., Keller, J., Angelidaki, I., Kalyuzhnyi, S. V., Pavlostathis, S. G., Rozzi, A., Sanders, W. T. M., Siegrist, H., & Vavilin, V. A. (2002). The IWA Anaerobic Digestion Model No 1 (ADM1). *Water Science and Technology*, *45*(10), 65–73. <https://doi.org/10.2166/wst.2002.0292>
- Batstone, D. J., Keller, J., & Blackall, L. L. (2004). The influence of substrate kinetics on the microbial community structure in granular anaerobic biomass. *Water Research*, *38*(6), 1390–1404. <https://doi.org/10.1016/j.watres.2003.12.003>
- Bergland, W. H., Dinamarca, C., & Bakke, R. (2015, October 7). *Temperature Effects in Anaerobic Digestion Modeling*. 56th Conference on Simulation and Modelling (SIMS 56), Linköping University, Sweden. <http://dx.doi.org/10.3384/ecp15119261>
- Buffière, P., Steyer, J.-P., Fonade, C., & Moletta, R. (1995). Comprehensive modeling of methanogenic biofilms in fluidized bed systems: Mass transfer limitations and multisubstrate aspects. *Biotechnology and Bioengineering*, *48*(6), 725–736. <https://doi.org/10.1002/bit.260480622>
- Coulson, J. M., & Richardson, J. F. (1999). *Chemical Engineering: Fluid flow, heat transfer and mass transfer* (Vol. 1). Pergamon Press.
- Cunha, J. R., Tervahauta, T., van der Weijden, R. D., Temmink, H., Hernández Leal, L., Zeeman, G., & Buisman, C. J. N. (2018). The Effect of Bioinduced Increased pH on the Enrichment of Calcium Phosphate in Granules during Anaerobic Treatment of Black Water. *Environmental Science & Technology*, *52*(22), 13144–13154. <https://doi.org/10.1021/acs.est.8b03502>
- Cussler, E. L. (1984). *Diffusion, mass transfer in fluid systems*. Cambridge University Press.
- Doloman, A., Mahajan, A., Pererva, Y., Flann, N. S., & Miller, C. D. (2020). A Model for Bioaugmented Anaerobic Granulation. *Frontiers in Microbiology*, *11*, 2239. <https://doi.org/10.3389/fmicb.2020.56682>
- Donoso-Bravo, A., Retamal, C., Carballa, M., Ruiz-Filippi, G., & Chamy, R. (2009). Influence of temperature on the hydrolysis, acidogenesis and methanogenesis in mesophilic anaerobic digestion: Parameter identification and modeling application. *Water Science and Technology*, *60*(1), 9–17. <https://doi.org/10.2166/wst.2009.316>
- Feldman, H., Flores-Alsina, X., Ramin, P., Kjellberg, K., Jeppsson, U., Batstone, D. J., & Gernaey, K. V. (2017). Modelling an industrial anaerobic granular reactor using a multi-scale approach. *Water Research*, *126*, 488–500. <https://doi.org/10.1016/j.watres.2017.09.033>
- Flora, J. R. V., Suidan, M. T., Biswas, P., & Sayles, G. D. (1995). A modeling study of anaerobic biofilm systems: I. Detailed biofilm modeling. *Biotechnology and Bioengineering*, *46*(1), 43–53. <https://doi.org/10.1002/bit.260460107>
- Henze, M., van Loosdrecht, M. C. M., Ekama, G. A., & Brdjanovic, D. (2008). *Biological Wastewater Treatment: Principles, Modelling and Design*. IWA Publishing. <https://doi.org/10.2166/9781780401867>
- Hofmann, A. F., Meysman, F. J. R., Soetaert, K., & Middelburg, J. J. (2008). A step-by-step procedure for pH model construction in aquatic systems. *Biogeosciences*, *5*(1), 227–251. <https://doi.org/10.5194/bg-5-227-2008>
- Hulshoff Pol, L. W., de Castro Lopes, S. I., Lettinga, G., & Lens, P. N. L. (2004). Anaerobic sludge granulation. *Water Research*, *38*(6), 1376–1389. <https://doi.org/10.1016/j.watres.2003.12.002>
- Kommedal, R., Bakke, R., Dockery, J., & Stoodley, P. (2001). Modelling production of extracellular polymeric substances in a

- Pseudomonas aeruginosa* chemostat culture. *Water Science and Technology*, 43(6), 129–134. <https://doi.org/10.2166/wst.2001.0357>
- Liu, Z., Yin, H., Dang, Z., & Liu, Y. (2014). Dissolved methane: A hurdle for anaerobic treatment of municipal wastewater. *Environmental Science & Technology*, 48(2), 889–890. <https://doi.org/10.1021/es405553j>
- Lohani, S. P., Wang, S., Bergland, W. H., Khanal, S. N., & Bakke, R. (2018). Modeling temperature effects in anaerobic digestion of domestic wastewater. *Water-Energy Nexus*, 1(1), 56–60. <https://doi.org/10.1016/j.wen.2018.07.001>
- Odrizola, M., López, I., & Borzacconi, L. (2016). Modeling granule development and reactor performance on anaerobic granular sludge reactors. *Journal of Environmental Chemical Engineering*, 4(2), 1615–1628. <https://doi.org/10.1016/j.jece.2016.01.040>
- Rebac, S., Ruskova, J., Gerbens, S., van Lier, J. B., Stams, A. J. M., & Lettinga, G. (1995). High-rate anaerobic treatment of wastewater under psychrophilic conditions. *Journal of Fermentation and Bioengineering*, 80(5), 499–506. [https://doi.org/10.1016/0922-338X\(96\)80926-3](https://doi.org/10.1016/0922-338X(96)80926-3)
- Reichert, P. (1994). AQUASIM – A Tool for Simulation and Data Analysis of Aquatic Systems. *Water Science and Technology*, 30(2), 21–30. <https://doi.org/10.2166/wst.1994.0025>
- Safitri, A. S., Michelle Kaster, K., & Kommedal, R. (2022). Effect of low temperature and municipal wastewater organic loading on anaerobic granule reactor performance. *Bioresource Technology*, 360, 127616. <https://doi.org/10.1016/j.biortech.2022.127616>
- Söllinger, A., & Urich, T. (2019). Methylotrophic methanogens everywhere—Physiology and ecology of novel players in global methane cycling. *Biochemical Society Transactions*, 47(6), 1895–1907. <https://doi.org/10.1042/BST20180565>
- Stewart, P. S. (1998). A review of experimental measurements of effective diffusive permeabilities and effective diffusion coefficients in biofilms. *Biotechnology and Bioengineering*, 59(3), 261–272. [https://doi.org/10.1002/\(SICI\)1097-0290\(19980805\)59:3<261::AID-BIT1>3.0.CO;2-9](https://doi.org/10.1002/(SICI)1097-0290(19980805)59:3<261::AID-BIT1>3.0.CO;2-9)
- Stewart, P. S., Hamilton, M. A., Goldstein, B. R., & Schneider, B. T. (1996). Modeling biocide action against biofilms. *Biotechnology and Bioengineering*, 49(4), 445–455. [https://doi.org/10.1002/\(SICI\)1097-0290\(19960220\)49:4<445::AID-BIT12>3.0.CO;2-9](https://doi.org/10.1002/(SICI)1097-0290(19960220)49:4<445::AID-BIT12>3.0.CO;2-9)
- Stewart Philip S. (2003). Diffusion in Biofilms. *Journal of Bacteriology*, 185(5), 1485–1491. <https://doi.org/10.1128/JB.185.5.1485-1491.2003>
- Sun, J., Dai, X., Wang, Q., Pan, Y., & Ni, B.-J. (2016). Modelling Methane Production and Sulfate Reduction in Anaerobic Granular Sludge Reactor with Ethanol as Electron Donor. *Scientific Reports*, 6(1), 35312. <https://doi.org/10.1038/srep35312>
- Wanner, O., & Gujer, W. (1986). A multispecies biofilm model. *Biotechnology and Bioengineering*, 28(3), 314–328. <https://doi.org/10.1002/bit.260280304>